Enhanced the luminescent performance of $CsPbI_3$ quantum dot-embedded borosilicate glass by controlling crystallization using Dy^{3+} ions as nucleating agent for remote color-tunable LEDs

Chaotong Zhou[1], Yu Ma[1], Fan Jiang[1], Guoying Zhao[1*], Jingshan Hou[1], Yufeng Liu[1], Xin Qiao[2*], Zhongzhi Wang[2], Ji-Guang Li[3], Yongzheng Fang[1*]

[1] *School of Materials Science and Engineering, Shanghai Institute of Technology, Shanghai 201418, PR China*

[2]*Baotou Research Institute of Rare Earths, Baotou, 014030, China*

[3]*Research Center for Functional Materials, National Institute for Materials Science, Tsukuba, Ibaraki 305-0044, Japan*

[*]*Corresponding author, E-mail addresses: zhaogy135@126.com; qiaoxinbt@163.com; fyz1003@sina.com.*

Abstract: Different concentrations of Dy^{3+} and perovskite quantum dots (PQDs) were simultaneously embedded in the B-Si-Zn glasses by melt-quenching and heat-treatment subsequently. A battery of experimental results including TEM, distribution of different elements, and photoluminescence prove that partial Dy ions are successfully doped into $CsPbI_3$ and played different roles depending on the doping concentration. When the Dy^{3+} concentration is circa 0.1mol%, Dy^{3+} as a nucleation agent reduces the energy required for the precipitation and growth of perovskite quantum dots, obtaining outstanding quantum efficiency of 31.82%. The excess Dy^{3+} supplement will prevent the mobility of PQDs elements. Based on the as-made glass sample, the remote fluorescent films have been successfully prepared. A kind of prototype lighting device was assembled, which demonstrated a high color rendering index of 96.5 under the current of 20mA. Interestingly, by adjusting the concentration of Dy^{3+}, color regulation can be achieved from orange-red light to yellow-white light.

Keywords: $CsPbI_3$; Dy^{3+}; Boron-silicate glass; Remote fluorescent films; High quantum efficiency

1. Introduction

In recent years, inorganic cesium lead halide ($CsPbX_3$, X=Cl, Br, I) perovskite quantum dots (PQDs) have attracted a lot of attention because of their excellent optical properties such as narrow full width at half maxima (FWHM), precisely tunable bandgap, large absorption intensity and high photoluminescence quantum yield (PLQY), which suggests great potential applications in optoelectronic fields including lighting, display as well as lasing[1-4]. Unfortunately, colloidal $CsPbX_3$ PQDs generally suffer from poor long-term stability upon the impact of moisture, heat and light irradiation of their low formation energy and ionic crystal features[5-7]. In previous studies, glass has become a well-regarded host for protecting perovskite quantum dots. The transparent glass matrix can cover the quantum dots, achieving good stability and maintaining the quantum dots excellent optical properties[8-10].

Different to the wet-chemical synthesis route to fabricate colloidal $CsPbX_3$ PQDs, the nucleation mechanism and growth behavior of quantum dots are greatly restricted by the properties of mother glass melt, though it protects them from environmental induced degradation[1,11,12]. During the heat treatment processing, the viscosity and rigidity of glass melt will hinder the mobility of Cs^+, Pb^{2+} and X^- ions, which make it difficult to obtain the whole-family precipitation of $CsPbX_3$ PQDs[13]. Consequently, how to realize controlled crystallization of quantum dots in glass remains challenging. Moreover, PLQYs of glass-stabilized $CsPbX_3$ PQDs are relatively lower than that of corresponding colloidal counterparts, especially $CsPbI_3$, which becomes a major issue to obstruct the practical application in solid-state lighting. To address this problem, Chen et al introduced F^- ions into borosilicate glass, obtaining PLQY of 50% from $CsPbI_3$[13]. Recently, the $CsPbI_3$ PQDs@glass has been prepared in our groups, and the highest PLQY value of glass stabilized $CsPbI_3$ reaches 17.1% by virtue of the regulation of glass grid structure[1]. It is reported that the PLQY of pure $CsPbI_3$ PQDs@glass is only 4.2%[14].

Another critical disadvantage of PQDs@glass is reabsorption between excitation and emission energy. In the current LEDs based on $CsPbX_3$ PQDs glass, it is necessary to mix different halogen synthesis glass powder to obtain a variety of multi-color converters by careful regulation[15]. In view of wide absorption band of $CsPbX_3$ PQDs, the energy transfer of excitation photons among different color glass powder is inevitable. In addition, it is difficult to obtain an appropriate proportion of $CsPbX_3$ PQDs in glass powder and ultimately get a white light via excitation by blue-chip, leading to a completely complicated and inefficient process[16,17]. The

existing technology is still not rid of the shortcomings of the dispensing LED package, such as complex operation and low efficiency[18]. Therefore, we need to synthesize a $CsPbX_3$ PQDs glass that can both effectively improve the operability and also enable better application in light-emitting diodes (LEDs). In this work, the remote fluorescent film of a single system has been successfully prepared for effectively solving the above problems.

From the above consideration, the rare earth ions, Dy^{3+} ions, were introduced into $CsPbI_3$ PQDs embedded borosilicate glasses in present work. The reasons for selecting Dy^{3+} ion are two-fold. Firstly, Dy^{3+} ion is a kind of glass network modifier, which can break the tightness of glass network, improving the mobility of extrusive Cs^+, Pb^{2+} and I^- ions during precipitation processing[1,19,20]. The homogeneous distribution of Dy^{3+} ion is beneficial to the finely controlled nucleation and growth of PQDs in glass host. Secondly, the yellow and blue color attributed to the f-f electronic transitions of Dy^{3+} ion will compensate colorimetric absence of $CsPbI_3$ PQDs, for the purpose of enhancing the luminescent performance[21,22]. By adjusting the concentration of Dy^{3+} dopants in glass matrix, the influence of Dy^{3+} dopants on structure and optical properties of $CsPbI_3$ PQDs has been systematically studied to explore its potential application in white LEDs. All the experimental results demonstrate that this Dy^{3+} doped glass-stabilized $CsPbI_3$ PQD characterized with high quantum efficiency, excellent physical/chemical stability and color tunability is a promising converter candidate for remote white LEDs.

2. Experimental Section

Glass specimens with the nominal composition of $38SiO_2$-$29B_2O_3$-$16ZnO$-$9Cs_2CO_3$-$5.4PbI_2$-$10.8KI$-xDy_2O_3 (x=0，0.1，0.3，0.5，0.7，0.8，1.0 mol%) were prepared by conventional melt-quenching. The raw materials were prepared from high-purity SiO_2，B_2O_3，ZnO，Cs_2CO_3，PbI_2，KI and Dy_2O_3 powder. Well-mixed raw materials (15 g) were dissolved in a capped alumina crucible and melted at 1200℃ for 15 min under an ambient atmosphere. Then the molten glass liquid was poured into a preheated copper plate to obtain precursor glass. Furthermore, the $CsPbI_3$ PQDs@glass was successfully prepared through controllable in-situ glass crystallization via heating at 480℃ for 10 h. Finally，the as-prepared glass samples were ground or polished to obtain a shape of 20×15×1.5 mm^3 for subsequent characterization.

The XRD patterns of the samples were recorded by X-ray diffraction (XRD) system (Rigaku, Ultima IV, Japan) through a Cu K_α radiation source with a scan range

covered from 10 to 80° and a scan rate of 8°/min and 0.02°/step. The microstructure of the sample was studied by TEM (JEM-2100F). The optical absorption spectra were recorded at room temperature using a UV–visible–NIR spectrophotometer (Hitachi, UH4150), working at 400–1800 nm. The photoluminescence properties (excitation spectra, emission spectra, and temperature dependent photoluminescence spectra) were measured by F-7000 spectrofluorometer equipped from Hitachi Instruments. PLQY and fluorescent lifetime for the $CsPbI_3$ PQDs@glass samples were recorded on an Edinburgh Instruments FS5 spectrofluorometer. All measurements were carried out at room temperature. The color of emission light was determined by CIE 1931 (x, y) chromaticity diagram.

Absolute photoluminescence Quantum yield (PLQY), defined as the ratio of emitted photons to absorbed ones, was measured by a spectrofluoremeter (FS5). An integrating sphere was mounted on the spectrofluoremeter with the entrance and exit ports located in 90° geometry. The PQD sample was located in the center of the integrating sphere. All the recorded spectroscopic data were corrected for the spectral responses of both the spectrofluoremeter and the integrating sphere. The responses of the detecting systems (integrating sphere, monochromators and detectors) in photon flux were determined using a calibrated tungsten lamp. Based on this setup, PLQY is calculated based on the following equitation

$$\eta = \frac{\text{number of photons emitted}}{\text{number of photons absorbed}} = \frac{L_{sample}}{E_{reference} - E_{sample}} \qquad (2\text{-}1)$$

where η represents QY, L_{sample} the emission intensity, $E_{reference}$ and E_{sample} the intensities of the excitation light not absorbed by the reference and the sample respectively. The difference in integrated areas between the sample and the reference represents the number of the absorbed photons. The emitted photons were determined by integrating the related emission band.

3. Result and Discussion

3.1 Crystal structure identification

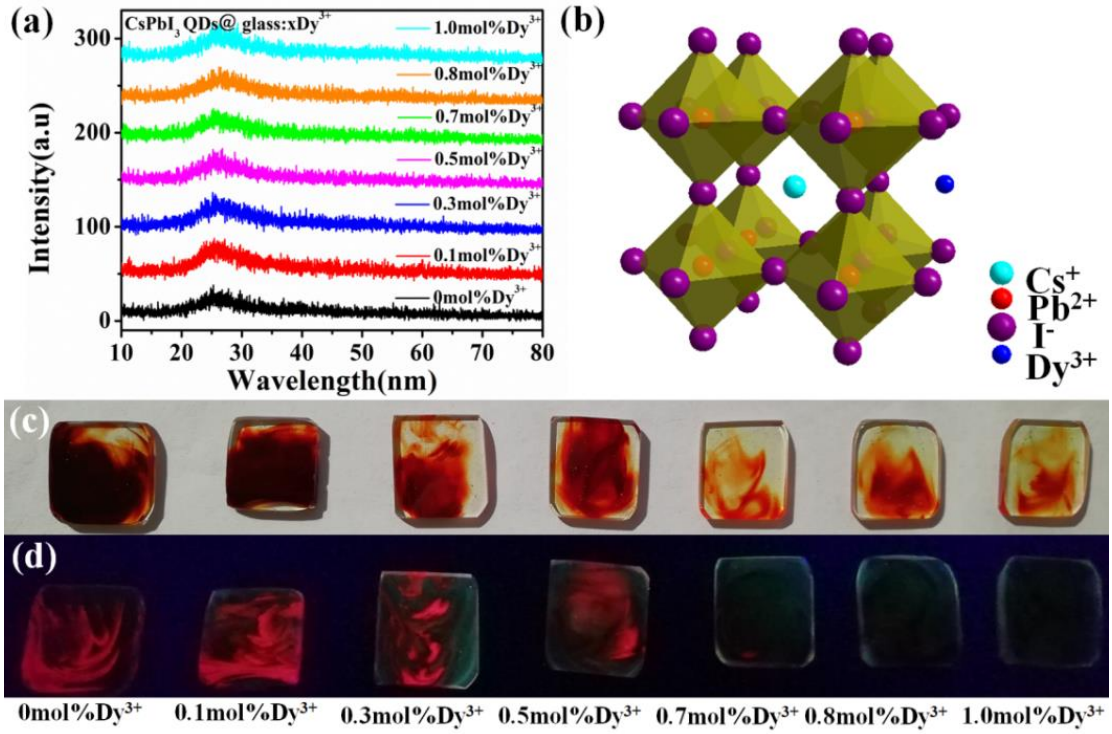

Figure 1. (a) XRD patterns of $CsPbI_3$ PQD@glasses with different Dy^{3+} ion doping concentrations; (b) crystal structure of $CsPbI_3$ PQD typical unit cell and the substitution of Dy^{3+}; (c) photographs of $CsPbI_3$ PQDs@glass plates with different Dy^{3+} ion doping concentrations under daylight and (d) irradiation of a UV lamp.

XRD patterns of a series of $CsPbI_3$ embedded glass with different concentrations of Dy^{3+} are shown in Figure 1a. Evidently, the patterns exhibit a broad hump in the diffraction angle of 26°, indicating that the typical amorphous feature of glass samples [23,24]. No obvious diffraction peaks attributed to $CsPbI_3$ PQDs are observed in XRD patterns, which might be due to the trace amount of quantum dots embedded within glasses[1,25,26]. Fortunately, the bright red color of glass flakes under an ultraviolet lamp confirms the successful precipitation of $CsPbI_3$ PQDs in glass (Figure 1c). In fact, there is a faint yellow light under the naked eye, but due to the low doping concentration of Dy, the luminous efficiency is hardly high. By contrast，the light from quantum dots is more concentrated and sharper, therefore，it appears red in the glass eventually. Figure.1b demonstrates the unit-cell structure of the $CsPbI_3$ PQD. It consists of 12-coordinated Cs^+ ions and 6-fold coordinated Pb^{2+} ions. With the increasing doping concentration of Dy^{3+} ions, the color of glass samples changed remarkably as shown in Figure 1c and d. It is indicated that the ligand surrounding Dy^{3+} ions has an important impact on the growth and photoluminescent behavior of

$CsPbI_3$ PQD.

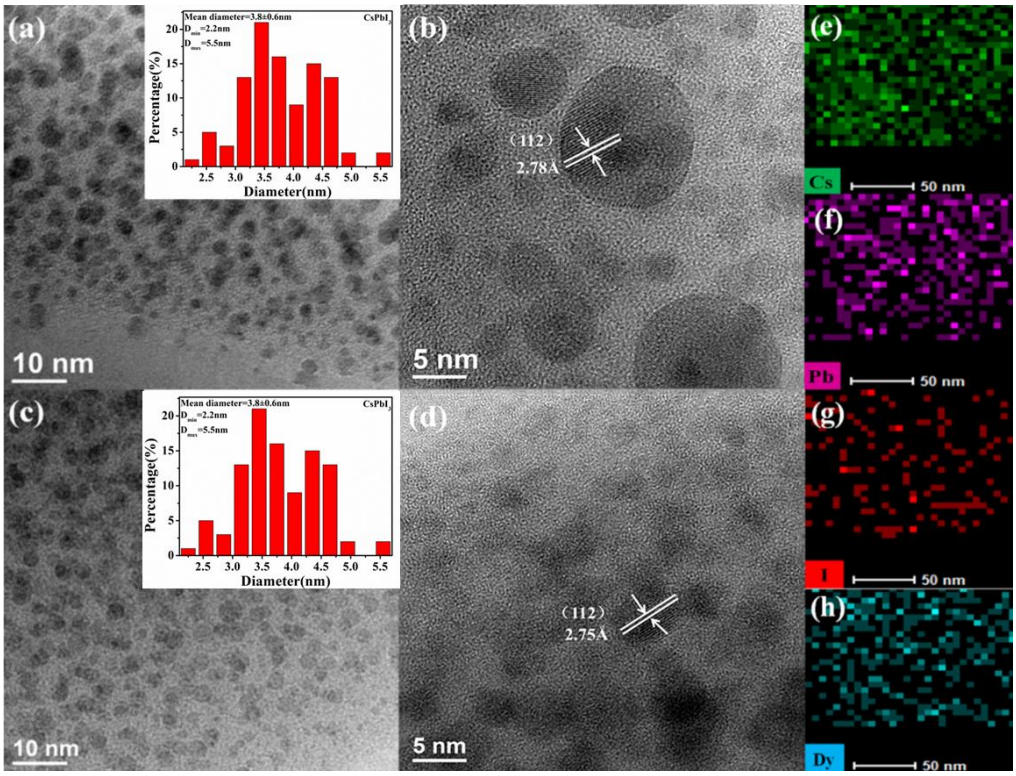

Figure 2. HRTEM spectra of $CsPbI_3$ QDs glass without Dy^{3+} (a, b) and with 0.5 mol% Dy^{3+} doping (c, d); the inset of (a) and (c): the particle size distribution for $CsPbI_3$ PQDs in the glass without Dy^{3+} and with 0.5 mol% Dy^{3+} doping, respectively; (e-h) Cs, Pb, I, Dy elemental mappings.

In order to further explore the existential state of Dy^{3+} ions in glass, high-resolution TEM (HRTEM) images of $CsPbI_3$ QDs glass without and with 0.5 mol% Dy^{3+} doped samples are depicted in Figure 2. The clear lattice fringes with an inter-planar distance of 2.78 Å evidence the successful precipitation of $CsPbI_3$ PQDs with high-crystallinity, which corresponds to the (112) crystal facet. This value of $CsPbI_3$ PQDs is decreased to 2.75 Å since the introduction of 0.5 mol% Dy^{3+} into glass matrix. The ionic radius of Dy^{3+} in 6-fold coordination is 0.912 Å suggesting substitution at Pb^{2+} (1.19 Å) sites in $CsPbI_3$ PQD[27]. The much big size difference between Dy^{3+} and Pb^{2+} in octahedral coordination gives reasonable evidence for the reduced inter-planar distance of (112) crystal facet. Notably, Figure 2a demonstrates the homogeneous distribution of PQDs with an average diameter of 3.8 nm. After the introduction of Dy^{3+}, the average diameter of PQDs was decreased to 3.4 nm in Figure 2c. By comparison, the spot size in Figure 2c exhibits the relatively regular distribution in Dy^{3+} ions doped glass sample.

The EDS mapping that includes Cs, Pb, I and Dy elements were carried out to

check the possible reaction between quantum dots and rare earth ions, as shown in Figure 2e-h. It is clearly seen that these elements are homogeneously dispersed in host glass. Nevertheless, the evidence that the overlap of the element distribution between Dy and I is comparatively small manifests that partial Dy^{3+} ions are involved in $CsPbI_3$ PQDs synthesis inevitably. As a result, there are two kinds of quantum dots in glass host, that is, $CsPbI_3$ and $CsDyI_3$. Dy_2O_3 as raw material is a glass network modifier, which can break the chemical bonds of bridging oxygens during the glass network forming processing. Therefore, the destruction of the ligand surrounding around reduces the energy required for the precipitation of all elements, promoting the formation of quantum dots [13,28]. Notably, the introduction of excessive Dy^{3+} supplements in raw material will limit the growth of PQDs in glass. Dy^{3+} ions seem to be an obstacle in the transmitting tunnel of all PQD elements. This can be explained by the adverse impact of Dy^{3+} for the surrounding elements polymerization, leading to hindering the mobility of extrusive Cs^+, Pb^{2+} and I^- ions from grid. Besides, the homogeneous distribution of Dy^{3+} in glass host is beneficial to guide to regular arrangement of quantum dots.

3.2 Luminescence Properties

In order to clarify the fluorescence property of $CsPbI_3$ QDs glasses doped with different concentrations of Dy^{3+}, the absorption and emission spectra were examined and shown in Figure 3a-b, respectively. The absorption spectra of glass samples have five sharp absorption peaks located at 800 nm, 896 nm, 1088 nm, 1271 nm and 1675 nm, which are characteristic absorption peaks of rare earth ion Dy^{3+}[20]. Moreover, a wide absorption band peaked around 680 nm is attributed to $CsPbI_3$ PQDs[29]. Interestingly, the absorption cut-off edge is detected to shift to the ultraviolet sideband with the increasing Dy^{3+} concentration, which is probably associated with the lower PQDs concentration resulting from the inhibiting effect aroused by excessive Dy^{3+} ions. Figure 2b exhibits the photoluminescence (PL) spectra of as-made samples under excitation at 365 nm. Three emission peaks can be easily seen from PL spectra except for the un-doped sample. The blue emission band peaked at 484 nm and yellow emission band peaked at 576 nm are attributed to the 4f-4f electronic transition $^4F_{9/2}\rightarrow{}^6H_{15/2}$ and $^4F_{9/2}\rightarrow{}^6H_{13/2}$ of Dy^{3+} ions, respectively. Besides, the red emission band around 620-650 nm originates from direct exciton recombination[12]. Except for the sample doped with 0.1 mol% Dy^{3+} ions, the peak wavelength of red emission shift towards the shorter wavelength side until it nearly quenches as the concentration of Dy^{3+} increases. Meanwhile, the intensity of red emission exhibits a similar change

tendency. Based on the above discussion, both sides of the introduction of Dy^{3+} ions into glass system should be responsible for this phenomenon. It is reasonable to conclude that there exists an optimal concentration of Dy^{3+} ions around 0.1 mol% in glass, which can boost the migration of PQDs element by loosening the glass grid. Dy^{3+} ion as glass network modifier breaks the bridging oxygen's links, as a result, reduces the energy required for precipitation and nucleation of $CsPbI_3$ PQDs[1,13].

The PL spectra reveal that the optimal Dy^{3+} doping concentration is circa 0.1 mol%. Correspondingly, the PLQY results also support this finding. Figure 3c exhibits the quantitative emission spectra of 0.1 mol% Dy^{3+} $CsPbI_3$ quantum dot glass and the reference sample and the corresponding absolute quantum yield, which was measured at an excitation wavelength of 365nm. The dependence of absolute PLQY values on the Dy_2O_3 content was recorded, as shown in Figure 3c, which has a similar tendency with $CsPbI_3$ QDs luminescence intensity. When Dy concentration is 0.1 mol%, the PLQY of red emission from PQDs embedded glass reaches the maximum value that is 31.82%. The excess Dy offer results in a drop of PLQY, which further evidences our insights of both sides. A similar change has also been detected in PL decay curve measurements (Figure 3d). To gain more understanding of the ligand surrounding Dy^{3+} in glass, the yellow-blue emission intensity (Y/B) ratio of Dy^{3+} was calculated and exhibited in the inset of Figure 3c. The $^4F_{9/2}\rightarrow{}^6H_{13/2}$ (yellow) transition is electric dipole (ED) transition and hypersensitive in nature, while the $^4F_{9/2}\rightarrow{}^6H_{15/2}$ (blue) transition is magnetic dipole (MD) dominant. The intensity ratio of electric dipole to magnetic dipole transitions has been used to measure the asymmetry and degree of covalence of the local environment of Dy^{3+} ions[30,31]. With the increasing Dy^{3+}concentration, Y/B ratio roughly exhibits the increasing trend. A twofold increase suggests the great change in ligand environment surrounding Dy^{3+} ions. It can be concluded that a great number of Dy^{3+} ions are located inside the distorted iodine octahedron, resulting in the formation of $CsDyI_3$. The regular structure of quantum dot and low covalence state of Dy^{3+}-I^- should be responsible for the low Y/B ratio when the concentration of Dy^{3+} ion in glass is 0.1 mol%. After the excess amount of Dy^{3+} ions were introduced into glass system, the structural tolerance capacity and low content of perovskite quantum dot drive the doped Dy^{3+} into amorphous phase. As a result, Y/B ratio is increased. Figure 3d exhibits the decay curves of $CsPbI_3$ PQDs in glasses, Nanosecond lifetime confirmed the typical exciton recombination characteristics of $CsPbI_3$ PQDs embedded in glass.

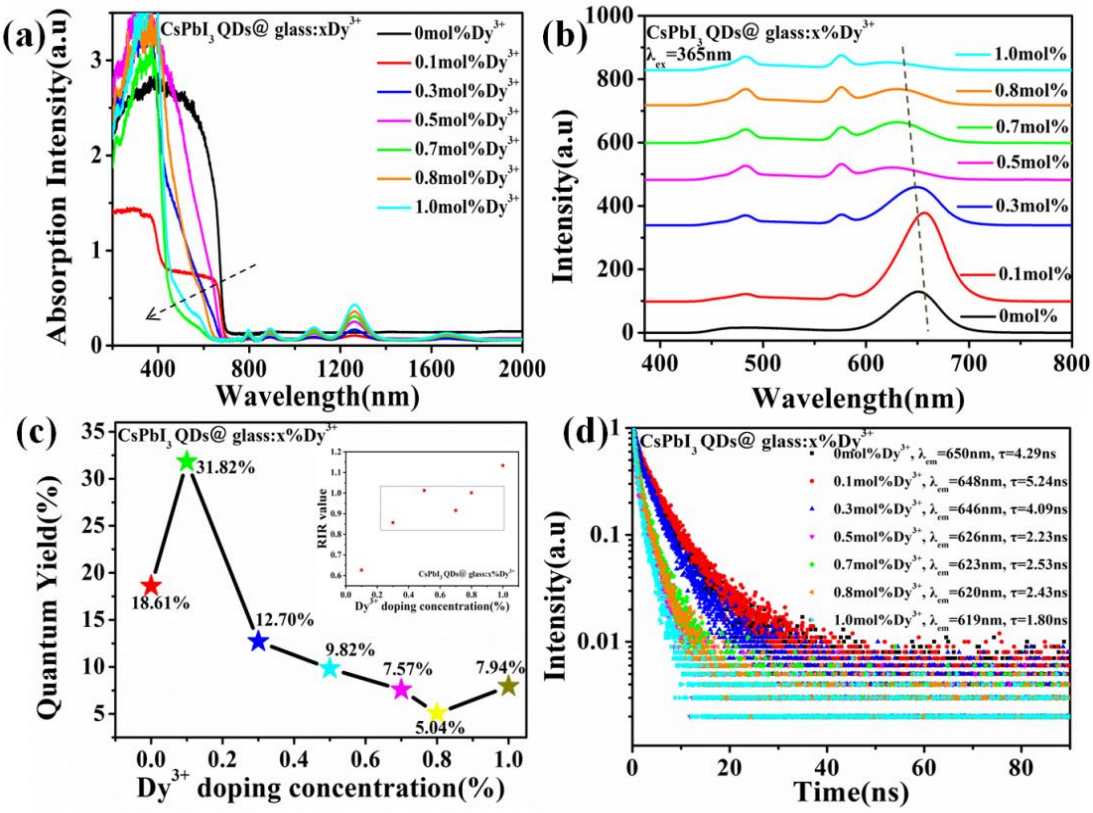

Figure 3. (a) Absorption spectra of $CsPbI_3$ QDs glasses doped with different concentrations of Dy^{3+}. The illustration shows the amplified absorption spectra near 690 nm (b) Emission spectra of glass samples excited by ultraviolet light at 365 nm. (c) The corresponding absolute quantum yield of $CsPbI_3$ PQDs glass doped with different concentrations of Dy^{3+} under excitation at 365 nm. Inset: the RIR value of $CsPbI_3$ QDs glasses doped with different concentrations of Dy^{3+}. (d) Fluorescence attenuation curves of monitored wavelengths at 620-650 nm under excitation at 365 nm.

3.3 Thermal and moisture stabilities

Poor stability is a major problem which limits the use of $CsPbI_3$ quantum dots in different applications[32]. The samples were tested for stability and Figure 4a presents the temperature-dependent PL spectra of glass sample measured at an excitation of 365 nm. It can be seen that there is no obvious change of the two characteristic peaks of Dy^{3+} with the temperature rise to 200 from 25℃, but the emission intensity of $CsPbI_3$ PQDs decreases continuously, which is due to the non-radiative transition and lattice relaxation of the luminescence center. Interestingly, as shown in Figure 4b, the intensity of luminescence recovered gradually until it was 82% of its initial intensity as temperature dropped. In addition, the moisture resistance test results showed that the location and intensity of emission peaks of glass sample had little change after 60 days (Figure 4c) The integral intensity of PL peak only decreased by less than 5% (Figure 4d), and luminance and color also was no significant change (Figure 4e). Similarly, PLQY is measured as 9.82% for day 0 and 9.79% for day 60 revealing very

close values. Therefore, it can be concluded that an inorganic glass host is indeed beneficial to efficiently protect PQDs from decomposition by water. In summary, it is borosilicate zinc glass matrix that improves remarkably the thermal stability and moisture resistance of Dy^{3+} doped $CsPbI_3$ PQDs.

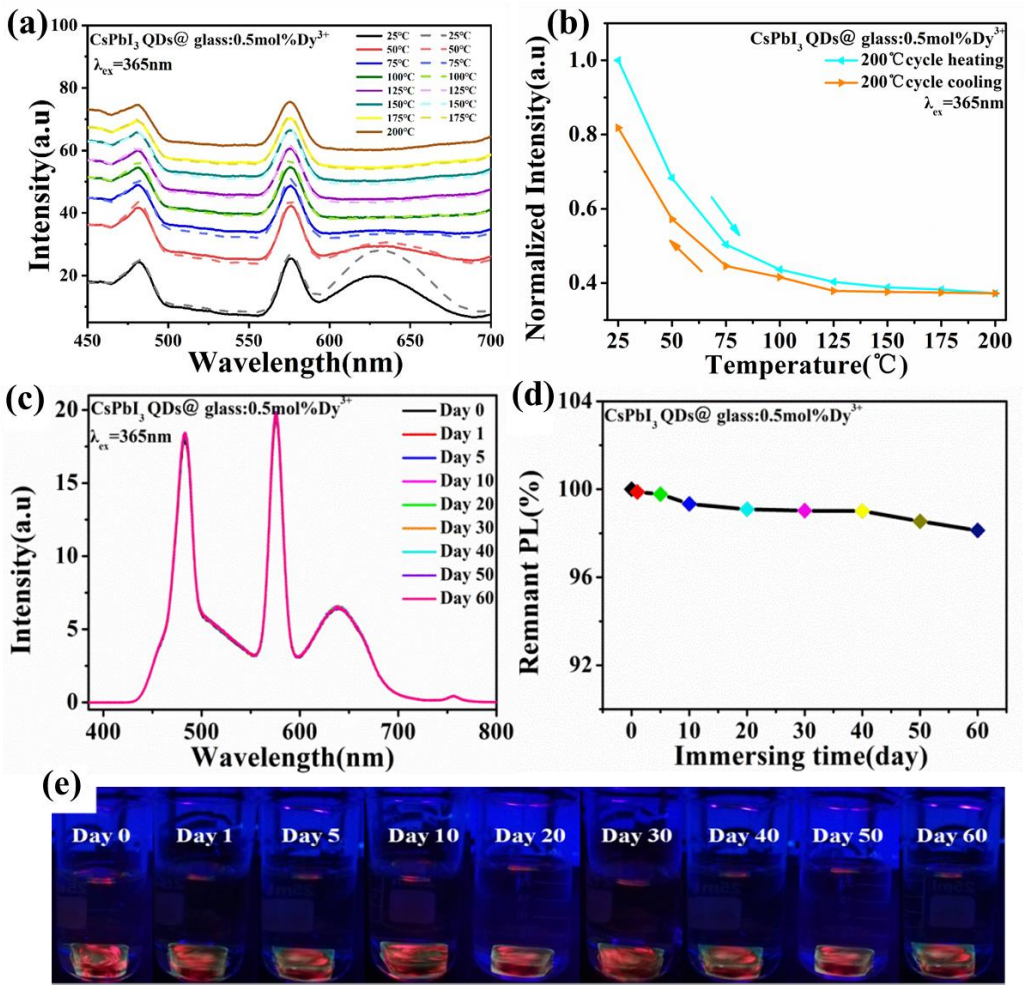

Figure 4. (a) $CsPbI_3$: temperature-dependent fluorescence spectra of Dy^{3+} perovskite quantum dot glass in the range of 25-200℃ under excitation at 365 nm; (b) $CsPbI_3$: Heating and cooling cycle of emission strength of Dy^{3+} perovskite quantum dot glass from 25℃ to 200℃.(c) PL spectrum of Dy^{3+} doped $CsPbI_3$ perovskite quantum dot glass irradiated by UV lamp at 365 nm during immersion in water for 60 days; (d) The variation of the integral intensity of peak PL with time; (e) Photoluminescence photos of Dy^{3+} doped $CsPbI_3$ perovskite quantum dot glass under the irradiation of 365 nm UV lamp during immersion in water for 60 days

3.4. CIE chromaticity coordinates and light-emitting devices

Due to the excellent optical properties and stability of the prepared Dy-doped $CsPbI_3$ PQDs@glasses, we consider it may have potential application in W-LEDs[33]. It is well known that the most common way to produce W-LEDs is to combine a yellow-emitting yttrium aluminum garnet phosphor with a blue-emitting LED chip[34].

This is inconvenient for the human eye to recognize the original color of the object due to its lack of a red-emitting portion[35]. In this work, we prepared Dy-doped $CsPbI_3$ PQDs@glasses, which can be used as a supplement to red light emission. A series of fluorescent glass films of $CsPbI_3$ PQDs with different dysprosium concentrations are prepared. The prepared glass samples of Dy^{3+} doped $CsPbI_3$ quantum dots were ground into powders and dispersed in a uniform mixture of solvents which is terpineol and ethyl cellulose ten to one in a certain proportion prepared a non-precipitating and uniform fluorescent slurry. Subsequently, the fluorescent paste was then evenly applied to the round glass substrate by a rotary coating method. Ultimately, the fluorescent glass film was prepared by drying the organic matter to completely volatilize for 3 hours in a draught drying cabinet at 150℃ (Figure. 5a). As shown in Figure 5b, it is can be seen the color of the glass film gradually changes under UV light. Noteworthy, when the doping concentration of Dy^{3+} is 0.5 mol%, the color of the glass changes into yellowish-white, manifesting that the as-prepared samples can be applied to W-LED. Therefore, the as-prepared Dy-doped $CsPbI_3$ PQDs@glass was combined with a UV chip to construct a W-LED device (Figure. 5c). Then the photoelectric properties of the LED devices were measured at a current of 20 mA. Besides, the color of these light-emitting diodes changes from red to yellow-green, and it can be certified in the CIE color coordinate diagram (Figure. 5d). The locus of $CsPbI_3$:0.5 mol% Dy^{3+} glass sample were in a blackbody radiance curve emitting dazzling white light. The corresponding CIE coordinates (x, y), correlated color temperature (CCT), color rendering index (CRI) and purity are listed in Table 1. Therefore, by modifying the content of Dy in the $CsPbI_3$ PQDs glass sample, the optical parameter can be easily tuned to find the best W-LED. The excellent performance of the W-LED device indicates that the as-prepared $CsPbI_3$ PQDs glass has potential applications in solid-state lighting and display[36].

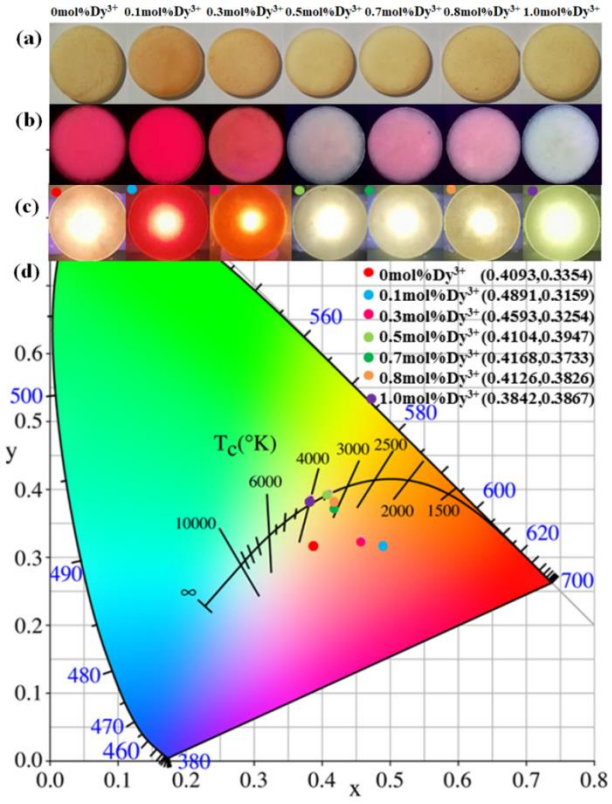

Figure 5. (a) $CsPbI_3$ PQDs fluorescent glass films with different Dy^{3+} doping concentrations;(b) a photograph of it under an ultraviolet lamp;(c) Light emitting photos of the prepared white LED devices;(d) CIE color coordinates

Table **1** Optical performance devices of white LED devices with different Dy^{3+} concentrations

Dy_2O_3 Concentration (mol%)	CIE coordinates	CCT (K)	CRI	Purity (%)
0	(0.4093,0.3354)	2874	52.9	23.4
0.1	(0.4891,0.3159)	1676	29.3	41.5
0.3	(0.4593,0.3254)	2015	6.6	35.4
0.5	(0.4104,0.3947)	3423	86.6	41.6
0.7	(0.4168,0.3733)	3104	89.7	37.1
0.8	(0.4126,0.3826)	3273	95.6	38.7
1.0	(0.3842,0.3867)	3974	69.7	31.4

4. Conclusion

In summary, Dy^{3+}-doped borosilicate glasses embedding $CsPbI_3$ PQDs were successfully prepared by a conventional melt quenching method, and the effect of Dy on optical properties of $CsPbI_3$ quantum dots has been investigated systematically. The TEM measurements verified that Dy^{3+} doped $CsPbI_3$ quantum dots are uniformly distributed in the glass. Since the increase of Dy^{3+} doping, the average size of $CsPbI_3$

PQDs is reduced, leading to blue shift of absorption cut-off wavelength and emission peak. The element distribution diagram shows that a part of Dy^{3+} exists the lattice of $CsPbI_3$ quantum dots, which promotes the formation of $CsPbI_3$ QDs. The effect of excessive Dy doping is opposite. The fluorescence spectrum revealed that the doping concentration circa 0.1 mol% is conducive to the generation of quantum dots, and the maximum quantum efficiency of 31.8% is obtained. Most importantly, benefiting from the remarkable optical performance and thermal stability, a simple W-LED was fabricated by combining UV chips based on the remote Dy^{3+} doped $CsPbI_3$ PQDs glass film, which demonstrated outstanding CRI of 95.6 at an operating current of 20 mA. By modifying the content of Dy in the $CsPbI_3$ PQDs glass sample, the color of simple W-LED can be easily modified without the other photoluminescent matrial system. This work exploits a new strategy to prepare high-performance $CsPbI_3$ PQDs glass and provides an interesting insight to develop their practical applications in solid state lighting and display.

Acknowledgement

Yongzheng Fang acknowledges financial supported by the the National Key Research and Development Program of China (Grant No. 2021YFB3500500). Guoying Zhao acknowledges financial supported by Science and Technology Talents Development Fund for Young Middle-aged Teachers Fund, Collaborative Innovation Fund (No. XTCX2022-03) of Shanghai Institute of Technology and Development of key technologies for the preparation and application of high-performance rare earth fluorescent block materials (No. BFXT-2022-D0046).

References:

[1] Qi F, Shao X, Ma Y, et al. Improved luminescent performances of $CsPbI_3$ perovskite quantum dots via optimizing the proportion of boron-silicate glass and precipitation processing[J]. Optical Materials, 2022, 124: 111981.

[2] Huang X, Guo Q, Yang D, et al. Reversible 3D laser printing of perovskite quantum dots inside a transparent medium[J]. Nature Photonics, 2020, 14(2): 82-88.

[3] Lin J, Lu Y, Li X, et al. Perovskite Quantum Dots Glasses Based Backlit Displays[J]. ACS Energy Letters, 2021, 6(2): 519-528.

[4] Peng Q, Wang T, Tang H, et al. Up- Converted Long Persistent Luminescence from $CsPbBr_3$ Nanocrystals in Glass[J]. Laser & Photonics Reviews, 2022: 2200449.

[5] Kim Y, Yassitepe E, Voznyy O, et al. Efficient luminescence from perovskite quantum dot solids[J]. ACS applied materials & interfaces, 2015, 7(45): 25007-25013.

[6] Liao M, Shan B, Li M. In situ Raman spectroscopic studies of thermal stability of all-inorganic cesium lead halide ($CsPbX_3$, X= Cl, Br, I) perovskite nanocrystals[J]. The journal of physical chemistry letters, 2019, 10(6): 1217-1225.
[7] Ye Y, Zhang W, Zhao Z, et al. Highly luminescent cesium lead halide perovskite nanocrystals stabilized in glasses for light- emitting applications[J]. Advanced Optical Materials, 2019, 7(9): 1801663.
[8] Yuan R, Shen L, Shen C, et al. $CsPbBr_3$: xEu^{3+} perovskite QD borosilicate glass: a new member of the luminescent material family[J]. Chemical communications, 2018, 54(27): 3395-3398.
[9] Chen D, Yuan S, Chen X, et al. $CsPbX_3$ (X= Br, I) perovskite quantum dot embedded low-melting phosphosilicate glasses: controllable crystallization, thermal stability and tunable emissions[J]. Journal of Materials Chemistry C, 2018, 6(25): 6832-6839.
[10] Ai B, Liu C, Wang J, et al. Precipitation and optical properties of $CsPbBr_3$ quantum dots in phosphate glasses[J]. Journal of the American Ceramic Society, 2016, 99(9): 2875-2877.
[11] Li X, Yu Y, Hong J, et al. Optical temperature sensing of Eu^{3+}-doped oxyhalide glasses containing $CsPbBr_3$ perovskite quantum dots[J]. Journal of Luminescence, 2020, 219: 116897.
[12] Chen D, Yuan S, Chen J, et al. Robust $CsPbX_3$ (X = Cl, Br, and I) perovskite quantum dot embedded glasses: nanocrystallization, improved stability and visible full-spectral tunable emissions[J]. Journal of Materials Chemistry C, 2018.
[13] Chen D, Liu Y, Yang C, et al. Promoting photoluminescence quantum yields of glass-stabilized $CsPbX_3$ (X = Cl, Br, I) perovskite quantum dots through fluorine doping[J]. Nanoscale, 2019, 11(37): 17216-17221.
[14] Liu S, Luo Y, He M, et al. Novel $CsPbI_3$ QDs glass with chemical stability and optical properties[J]. J Eur Ceram Soc, 2018, 38(4): 1998-2004.
[15] Kıbrıslı O, Erol E, Ersundu M Ç, et al. Robust $CsPbBr_3$ and CdSe/Dy^{3+}+ CdSe quantum dot doped glass nanocomposite hybrid coupling as color converter for solid-state lighting applications[J]. Chemical Engineering Journal, 2021, 420: 130542.
[16] Wang Z, Shen X, Tang C, et al. Efficient and Stable CF_3PEAI-Passivated $CsPbI_3$ QDs toward Red LEDs[J]. ACS Applied Materials & Interfaces, 2022, 14(6): 8235-8242.
[17] Xie B, Hu R, Luo X. Quantum dots-converted light-emitting diodes packaging for lighting and display: status and perspectives[J]. Journal of Electronic Packaging, 2016, 138(2): 020803.
[18] Erol E, Kıbrıslı O, Ersundu M Ç, et al. Color tunable emission from Eu^{3+} and Tm^{3+} co-doped $CsPbBr_3$ quantum dot glass nanocomposites[J]. Physical Chemistry Chemical Physics, 2022, 24(3): 1486-1495.
[19] Zekri M, Herrmann A, Turki R, et al. Experimental and theoretical studies of Dy^{3+} doped alkaline earth aluminosilicate glasses[J]. Journal of Luminescence, 2019, 212: 354-360.
[20] Ma Y, Zhao G, Guo Y, et al. Structural characterization and photoluminescence properties of B_2O_3–Bi_2O_3–SiO_2 glass containing Dy^{3+} ions[J]. Journal of Luminescence, 2020, 227: 117591.
[21] Kim J S, Eswaran S K, Kwon O H, et al. Enhanced Luminescence Characteristics of Remote Yellow Silicate Phosphors Printed on Nanoscale Surface-Roughened Glass Substrates for White Light-Emitting Diodes[J]. Advanced Optical Materials, 2016, 4(7): 1081-1087.
[22] Erol E, Vahedigharehchopogh N, Ekim U, et al. Ultra-stable Eu^{3+}/Dy^{3+} co-doped CsPbBr3 quantum dot glass nanocomposites with tunable luminescence properties for phosphor-free WLED applications[J]. Journal of Alloys and Compounds, 2022, 909: 164650.

[23] Zheng R, Ueda J, Shinozaki K, et al. In Situ Growth Mechanism of $CsPbX_3$ (X= Cl, Br, and I) Quantum Dots in an Amorphous Oxide Matrix[J]. Chemistry of Materials, 2022, 34(4): 1599-1610.
[24] Zhao G, Xu L, Meng S, et al. Facile preparation of plasmon enhanced near-infrared photoluminescence of Er^{3+}-doped Bi_2O_3-B_2O_3-SiO_2 glass for optical fiber amplifier[J]. J Lumin, 2019, 206: 164-168.
[25] Reza Dousti M, Sahar M R, Rohani M S, et al. Nano-silver enhanced luminescence of Eu^{3+}-doped lead tellurite glass[J]. J Mol Struct, 2014, 1065-1066: 39-42.
[26] Dousti M R, Poirier G Y, Amjad R J, et al. Luminescence quenching versus enhancement in WO_3-$NaPO_3$ glasses doped with trivalent rare earth ions and containing silver nanoparticles[J]. Opt Mater, 2016, 60: 331-340.
[27] Zhu Y, Yang B, Lu Q, et al. Stable Dy-doped $CsPbBr_3$ quantum dot glass with enhanced optical performance[J]. Journal of Non-Crystalline Solids, 2022, 575: 121224.
[28] Li P, Duan Y, Lu Y, et al. Nanocrystalline structure control and tunable luminescence mechanism of Eu-doped $CsPbBr_3$ quantum dot glass for WLEDs[J]. Nanoscale, 2020, 12(12): 6630-6636.
[29] Lu C, Li H, Kolodziejski K, et al. Enhanced stabilization of inorganic cesium lead triiodide ($CsPbI_3$) perovskite quantum dots with tri-octylphosphine[J]. Nano Research, 2018, 11(2): 762-768.
[30] Shamshad L, Rooh G, Kirdsiri K, et al. Photoluminescence and white light generation behavior of lithium gadolinium silicoborate glasses[J]. Journal of Alloys and Compounds, 2017, 695: 2347-2355.
[31] Uma V, Maheshvaran K, Marimuthu K, et al. Structural and optical investigations on Dy^{3+} doped lithium tellurofluoroborate glasses for white light applications[J]. Journal of Luminescence, 2016, 176: 15-24.
[32] Erol E, Kıbrıslı O, Ersundu M Ç, et al. Size-controlled emission of long-time durable $CsPbBr_3$ perovskite quantum dots embedded tellurite glass nanocomposites[J]. Chemical Engineering Journal, 2020, 401: 126053.
[33] Yuan L, Zhou L, Xiang W, et al. Enhanced stability of red-emitting $CsPbI_3$: Yb^{3+} nanocrystal glasses: A potential luminescent material[J]. Journal of Non-Crystalline Solids, 2020, 545: 120232.
[34] Chen H-S, Hsu C-K, Hong H-Y. Ingan-cdse-znse quantum dots white LEDs[J]. Ieee photonics technology letters, 2005, 18(1): 193-195.
[35] Xuan T-T, Liu J-Q, Xie R-J, et al. Microwave-assisted synthesis of CdS/ZnS: Cu quantum dots for white light-emitting diodes with high color rendition[J]. Chemistry of Materials, 2015, 27(4): 1187-1193.
[36] Jiang J, Shao G, Zhang Z, et al. Ultrastability and color-tunability of $CsPb(Br/I)_3$ nanocrystals in P–Si–Zn glass for white LEDs[J]. Chemical Communications, 2018, 54(87): 12302-12305.

CRediT authorship contribution statement

Chaotong Zhou: Conceptualization, Writing-original draft. **Yu Ma:** Data curation, Formal analysis. **Fan Jiang:** Methodology, Investigation. **Guoying Zhao:** Methodology, Investigation, Supervision. **Jingshan Hou:** Methodology, Investigation. **Yufeng Liu:** Methodology, Validation. **Xin Qiao:** Investigation, Writing - Review & Editing. **Zhongzhi Wang:** Resources. **Ji-Guang Li:** Funding acquisition. **Yongzheng Fang:** Supervision.

Declaration of interests

☑The authors declare that they have no known competing financial interests or personal relationships that could have appeared to influence the work reported in this paper.

☐The authors declare the following financial interests/personal relationships which may be considered as potential competing interests: